Length and Time-Dependent Rates in Diffusion-Controlled Reactions with Conjugated Polymers

Paiboon Sreearunothai,[†,‡] Sadayuki Asaoka,[§] Andrew R. Cook,[†] and John R. Miller*[,†]

Chemistry Department, Brookhaven National Laboratory, Upton, New York 11793–5000 and Chemical Resources Laboratory, Tokyo Institute of Technology, Yokohama, 226–8503, Japan

Received: October 23, 2008; Revised Manuscript Received: December 20, 2008

Rate constants for diffusion-controlled reactions of solvated electrons with conjugated fluorene oligomers (oF) and polymers (pF) were measured in liquid tetrahydrofuran (THF). Preparative gel permeation chromatography (GPC) was used to separate the polyfluorenes into fractions having narrowed distributions of lengths. Both oF and pF's were used in determinations of the attachment rate constants k_{inf} as a function of length, where k_{inf} refers to the rate coefficients at long times where they are indeed constant. The results find that in going from oF_1 to pF_{133}, k_{inf} increases by a factor of 16, which is much smaller than that of the 133-fold increase in length. The extent of this increase and its change with length are in excellent agreement with published theoretical models that describe diffusion to long thin objects as either prolate spheroids or one-dimensional arrays of spheres. As the concentration of polymer was increased, the effects of large transient terms in the rate constant were observed. As predicted by the Smoluchowski diffusion equation, with modifications by more contemporary theorists, these transient effects are larger and persist to longer times for the larger molecules. For the longest molecule, pF_{133}, $k(t)$ increases by more than a decade at short times. In that case, the "transient term" becomes dominant and the rate coefficient is approximately proportional to the square of the effective reaction radius in contrast to the linear dependence usual for diffusional reactions. The size of these transient effects and their quantitative confirmation are unprecedented.

Introduction

This paper is about diffusion-controlled reactions of molecules having lengths from 1 to over 100 nm. Classically diffusion-controlled reactions occur on every encounter of the reacting species, so the rate constants depend only on the diffusion coefficients and the reaction radius with little dependence on specific reactivities. The theory of Smoluchowski[6] produced an equation, the simple form of which has proved to be remarkably durable:

$$k(t) = 4\pi R_{eff} D N_A (1 + R_{eff}/(\pi D t)^{1/2}) \quad (1)$$

$$k_{inf} = 4\pi R_{eff} D N_A \quad (2)$$

Equation 1 gives the rate constant for a bimolecular, diffusion-controlled reaction in terms of just two parameters: the mutual diffusion coefficient, $D = (D_A + D_B)$, and the effective reaction radius, R_{eff}. R_{eff} has different meanings: (1) In the Smoluchowski[6] theory for diffusion-controlled reactions of small molecules approximated as spheres, R_{eff} is just the sum of the physical radii of the two reactants. The reaction rate at contact is taken as infinite and zero otherwise. Subsequent more precise theories developed many elaborated forms to deal with finite rate on contact,[7,8] and complexities that cause deviations from eq 1 have been reviewed.[9−11] (2) Electron transfer[12−14] and electronic energy transfer do not require physical contact for reaction and occur over a range of distances,[12−15] so R_{eff} is typically a few to several Å larger than the physical sizes of the reactants at ordinary viscosities. (3) Reactions with non-spherical molecules can be accommodated in the same framework with R_{eff} representing an average reaction distance. Recent theories can compute R_{eff} for diffusion of point particles (or spheres) to the surfaces of shapes including ellipsoids,[5] lines, planes, and cubes of spherical reactants.[3,4,16−23] The important changes to eq 1 contributed by many theoreticians have affected the sense and utility of what might be termed the "modified Smoluchowski equation". Although the change from R to R_{eff} is superficially simple, the developing meaning of R_{eff} represents a deeper evolution of our understanding.

Equation 1 additionally contains a "transient term". The rate coefficient is not constant but decreases with $t^{-1/2}$ at short times leveling off to the constant value, k_{inf}, in eq 2 at long times.[6,7,9] For reactions of small molecules in water or common nonaquous solvents, the transient term is significant only on the picosecond time scale.[8,24−26] For large molecules, the theories predict that R_{eff} and therefore k_{inf} can increase by factors of 10 or more. Larger R_{eff}'s also cause the effect of the transient term to persist to the nanosecond and even to the microsecond time scale.[27] Large rate constants and transient terms have been observed for reactions of holes, electrons, or triplets with conjugated polymers.[27−29] Once R_{eff} and the diffusion coefficient are known, eq 1 can be used to describe the time-dependent nature of the reaction rate.

The simple form of eq 1 is not exact. At times sufficiently short that diffusion is not a dominant contributor to the rate, nondiffusional tunneling kinetics at fixed geometries are dominant.[12,30,31] This paper examines reactions at somewhat longer times well into the diffusional regime. Here, eq 1 comprises the first two terms of a series[32] that converges rapidly. While eq 1 is known to have inherent failings at very short times and high concentrations, especially when combined with low diffusion constants,[10,11] it is the form recovered for electron

* To whom correspondence should be addressed.
[†] Chemistry Department, Brookhaven National Laboratory.
[‡] Present address: Sirindhorn International Institute of Technology, Thammasat University – Pathum Thani 12121, Thailand.
[§] Chemical Resources Laboratory, Tokyo Institute of Technology.

10.1021/jp809413x CCC: $40.75
Published on Web 03/04/2009

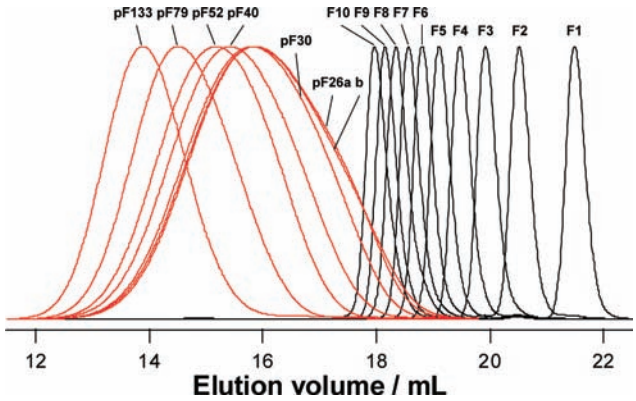

Figure 1. GPC profiles of oligofluorenes **F1**−**10** (black) and fractionally separated poly-2,7-(dihexylfluorene)s (red lines).

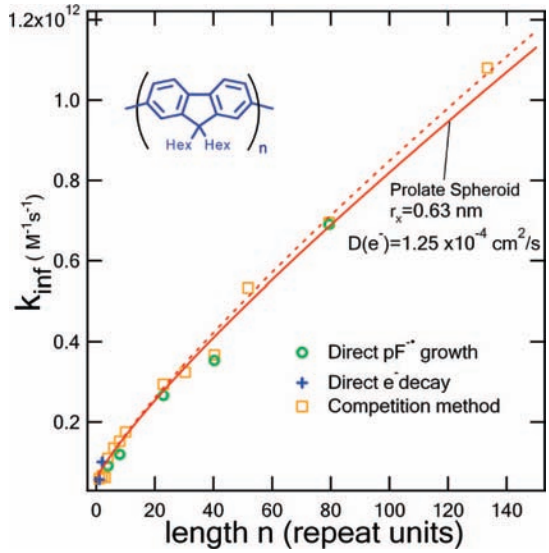

Figure 2. Rate constants for attachment of solvated electrons to oligo- and polyfluorenes in THF solution at 295 K. These rate constants were measured at low oF and pF concentrations to determine k_{inf}, the time-independent term in eq 1, by direct observation of $pF^{-\bullet}$ or $oF^{-\bullet}$ growth kinetics, direct observation of e_s^- decay kinetics, and competition with e_s^- capture by small molecules (DCE, DBM, and BuI). The results are compared with predictions in which the diffusion-controlled capture is modeled as the diffusional flux to a prolate spheroid[5] (eqs 2 and 5) with $D = D(e_s^-) + D(M)$, where $D(e_s^-) = 1.25 \times 10^{-4}$ cm^2/s and the much smaller diffusion coefficients of the molecules, $D(M)$, vary with length (see Table 2). The dashed line shows a fit with constant $D = 1.3 \times 10^{-4}$ cm^2/s that neglects variations with length.

transfer to small molecules[12,30,31] and for reactions of more extended objects[20,23,32] and was used in the first application to conjugated polymers.[27] For large molecules, the form of the transient term in eq 1 has been described as universal.[23] The large values of R_{eff} for polymeric molecules should extend the time dependence to longer times and make its shape more easily observable, but quantitative experimental tests are not yet available.

This paper reports measurements of reactions of solvated electrons with a series of oligo- and polyfluorenes pictured in Figure 2 that have up to 133 of the repeat units. These reactions are investigated to seek quantitative tests of theories that give R_{eff} as a function of length for long molecules. The characterization of these diffusion-controlled processes is described as two tasks. The first is to determine how k_{inf}, the time-independent rate constant at long time, depends on the length of the molecule. The second task is to characterize the transient term under conditions where it is large. The experimental data will be compared with two principal theoretical models that compute R_{eff} for electron capture by the long, conjugated polymers investigated here, that of a prolate spheroid and a line of spheres.

TABLE 1: Properties of pF Fractions

	GPC			GPC-MALLS	
	M_N[a]	M_W/M_N	n_{GPC}[b]	M_W[c]	n_{MALLS}[d]
pF[e]	19 500	2.30	32.4	24 800	31.4
PF$_{133}$	80 200	1.27	133.4	57 600	135.8
pF$_{79}$	47 700	1.39	79.4	39 000	83.5
pF$_{52}$	31 200	1.50	51.8	29 000	57.3
pF$_{40}$	24 200	1.60	40.3	24 700	45.3
pF$_{30}$	18 200	1.71	30.3	19 900	34.0
pF$_{23}$	13 800	1.89	22.9	18 500	28.4

[a] The number-averaged molecular weight by GPC relative to PS standards. [b] Length in repeat units determined by calibration with PS standards. [c] The absolute weight averaged molecular weight by GPC-MALLS analysis using a Debye plot. [d] Calculated from M_W, M_W/M_N, and the formula weight of a dihexylfluorene repeat unit. [e] Prior to separation.

Experimental Section

Chemicals. The reagents and solvents for synthesis were used as purchased from Aldrich. Tetrahydrofuran (THF) for pulse radiolysis was distilled from sodium-benzophenone under argon. ^{1}H NMR spectra were obtained with a Bruker 400 MHz spectrometer in chloroform-d. Gel permeation chromatography (GPC) analysis was carried out on a series connection of two ϕ7.8 × 300 mm TSK gel H_{XL}-M columns (Tosoh) thermostatted at 35 °C equipped with an ERC-8710 UV−vis (Erma) and an RI-101 RI (Shodex) detectors using THF as eluent. The number-averaged molecular weight (M_N) and polydispersity (M_W/M_N) were calculated by using a series of polystyrenes (PS, Aldrich) as calibration standard. Absolute molecular weights of pF were determined by GPC coupled to multiangle laser light scattering (GPC-MALLS) analysis on the GPC system equipped with a mini-DAWN Tristar (Wyatt Technology) detector. Preparative scale GPC was conducted by using an LC-9101 recycling preparative high performance liquid chromatography (HPLC) system (Japan Analytical Industry) equipped with a series connection of Jaigel-2H and 3H columns.

Oligofluorene Synthesis. A series of oligofluorenes, oF_n, having 1−10 fluorene units were synthesized according to the modified procedures reported by Geng et al.[33] and Tsolakis and Kallitsis.[34] Apparent number averaged molecular weights were calculated from GPC elution volumes by comparison to polystyrene standards. This calibration afforded an excellent linear relationship ($R^2 = 0.9985$) to the actual molecular weights.

Synthesis of Poly-2,7-(9,9-dihexylfluorene) (pF). Polyfluorene was prepared by polycondensation of 2,7-dibromo-9,9-dihexylfluorene (**F1Br$_2$**) according to the procedure reported by Klaerner and Miller.[35] 2-Bromofluorene was used as the end-capping reagent. In a Schlenk flask, bis(1,5-cyclooctadiene) nickel(0) (4 g, 15 mmol), 1,5-cyclooctadiene (1.8 mL, 15 mmol), and 2,2′-bipyridine (2.3 g, 15 mmol) were dissolved in the mixed solvent of toluene (80 mL) and dimethylformamide (DMF) (80 mL) and were heated at 80 °C for 30 min under an argon atmosphere. A toluene (60 mL) solution of **F1Br$_2$** (4 g, 8.1 mmol) and 2-bromofluorene (133 mg, 0.54 mmol) was added, and the reaction mixture was heated at 80 °C for 2 days and then was poured into an equivolume mixture of concentrated hydrochloric acid, methanol, and acetone. The organic layer was extracted with toluene, was washed with brine, and then was dried over Na_2SO_4. The solvent was removed under reduced

TABLE 2: Rate Constants in M^{-1} s^{-1} for Attachment of Solvated Electrons to Oligo and Polyfluorenes in THF at 295 K[a]

n[b]	k_{inf} direct[c]	k_{inf} comp[d]	pF conc. (μM) comp[e]	D(M)[f] cm^2/s	R_{eff}[g] nm
1	5.66×10^{10}	5.88×10^{10}	400	9.85×10^{-6}	0.58
2	9.99×10^{10}	6.62×10^{10}	200	6.5×10^{-6}	0.67
3		6.15×10^{10}	110	5.1×10^{-6}	0.63
4	9.05×10^{10}	1.09×10^{11}	890	4.29×10^{-6}	1.11
6		1.36×10^{11}	100	3.36×10^{-6}	1.40
8	1.19×10^{11}	1.52×10^{11}	100	2.83×10^{-6}	1.57
10		1.75×10^{11}	423	2.47×10^{-6}	1.82
23	2.66×10^{11}	2.94×10^{11}	100	1.5×10^{-6}	3.07
30		3.24×10^{11}	95	1.28×10^{-6}	3.39
40	3.53×10^{11}	3.67×10^{11}	100	1.08×10^{-6}	3.85
52		5.33×10^{11}	25	9.2×10^{-7}	5.60
79	6.91×10^{11}	6.95×10^{11}	64	7.16×10^{-7}	7.31
133		1.08×10^{12}	8	5.24×10^{-7}	11.37

[a] The rate constants were determined at low concentrations to obtain estimates of the long time limit, k_{inf}. [b] The number of repeat units in the oligomer or polymer. [c] Determined by decay of solvated electrons for $n = 1$ or 2 and by growth of $oF^{-\bullet}$ or $pF^{-\bullet}$ anions at three concentrations: 10, 25, and 50 μM for the longer molecules (average values reported). Uncertainty is $\pm 10\%$ for F_1. It is $\pm 25\%$ for F_2 because of overlap of absorption from F_2 anions. [d] Determined by competition with alkyl halides (see text); uncertainties are $\pm 15\%$. [e] Concentration of oligomer or polymer used in competition experiments; the competitor used was 1,2-dichloroethane (DCE) except for pF_{133} where 1-iodobutane (BuI) was used. [f] Diffusion coefficients for the molecules, estimated as $D_M = 1.13 \times 10^{-5}\ (0.75n/0.6)^{-0.6}$ cm^2/s, where n is the number of repeat units. This equation[74] was found[41] to provide a good description for measurements on oligomers[41] and polymers.[42] [g] R_{eff} calculated from k_{inf} (competition) using eq 1b with $D = D(e_s^-) + D(M)$; $D(e_s^-) = 1.25 \times 10^{-4}$ cm^2/s and D(M) as given in this table. The principal source of uncertainty in absolute values of R_{eff} is the 20% uncertainty in $D(e_s^-) = (1.25 \pm 0.25) \times 10^{-4}$. Relative values of R_{eff} for different lengths should be certain to $\pm 10\%$.

pressure, and the crude polymer was dissolved in a small amount of chloroform and was reprecipitated twice from methanol prior to Soxhlet extraction with acetone for 3 days to remove low molecular weight polymers to give ivory powder (2.5 g, 91% yield). ^{1}H NMR ($CDCl_3$) δ 0.76−0.81 (m, 10nH), 1.09−1.15 (m, 12nH), 2.12 (m, 4nH), 4.02 (s, 4H on 9-position of terminal-fluorene), 7.31−7.90 (m, 6nH). GPC $M_N = 19\,500$, $M_W/M_N = 2.30$ on the basis of PS standard. GPC-MALLS $M_W = 24\,800$.

The obtained pF was then fractionally separated with preparative scale GPC. The GPC profiles of pF fractions are shown in Figure 1. The number-averaged molecular weight (M_N) and polydispersity (M_W/M_N) of pF on the basis of PS standard are summarized in Table 1. Given the excellent linear agreement between predicted and known molecular weights for the oligofluorenes described above, it is possible to determine the averaged polymerization degrees (n_{GPC}) of the pF fractions by extrapolating the oF PS calibration plot to the observed M_N values. As a check, the average polymerization degrees were also calculated from the absolute molecular weight obtained by GPC-MALLS analysis, n_{MALLS}. The differences of the GPC and MALLS values were less than 5 repeat units.

Pulse Radiolysis. Electron attachment measurements were carried out at the Brookhaven National Laboratory Laser-Electron Accelerator Facility (LEAF). The LEAF facility and the methods used are described elsewhere[36−38] as are application to conjugated polymers.[28,29] Briefly, the electron pulse ($\leq$50 ps duration) was focused into a quartz cell with an optical path length of 20 mm containing the solution of interest under argon in purified tetrahydrofuran (THF) in an inert atmosphere glovebox. The monitoring light source was a pulsed xenon arc lamp. Wavelengths were selected using either 40 or 10 nm bandpass interference filters. Transient absorption signals were detected with either silicon (EG&G FND-100Q, $\leq$1000 nm) or InGaAs (GPD Optoelectronics GAP-500 L, $\geq$1100 nm) photodiodes or a biplanar phototube (Hamamatsu R1328U-03, $\leq$ 650 nm) and were digitized with a Lecroy 8620A. While most measurements have 2−4 ns time resolution, 125 ps system risetime is attained in the visible using the biplanar phototube and short path cells.

Results and Discussion

1. Determination of k_{inf} as a Function of Molecule Length. The reaction investigated is the attachment of solvated electrons (e_s^-) to 1−10 unit long oligofluorenes (oF) and 23−133 unit long polyfluorenes (pF) in THF solvent. The solvated electron in THF is a powerful reducing agent making it likely that attachment will be diffusion-controlled. Upon ionization of THF, e_s^- is formed in less than 1 ps;[39] the rapid formation is useful for investigations of time dependence of eq 1. Its diffusion coefficient, $D(e_s^-)$, has been determined as 0.77,[2] 1.35,[1] and $1.37^1 \times 10^{-4}$ cm^2/s. An additional value, 1.35×10^{-4} cm^2/s, is obtained from the 7.9×10^{11} M^{-1} s^{-1} rate constant[40] for electron capture by Na^+ and the Debye−Smoluchowski equation. The mean (rms) of these values $D(e_s^-) = (1.25 \pm 0.25) \times 10^{-4}$ will be utilized here. Diffusion coefficients of the oF and pF molecules are much smaller. Reported values vary from 5.2×10^{-6} (oF_3)[41] to 4×10^{-7} ($pF_{\sim 140}$).[42] They are described well[41] by a form proposed by Yamakawa.[74] D(M) from that form are given in Table 2. Table 2 also lists and Figure 2 plots the observed e_s^- attachment rate constants determined at low concentrations of oligo- and polyfluorenes as a function of the number of fluorene repeat units, n. Measurements were made using a combination of direct and indirect techniques described below. Table 2 also gives values of the effective (spherical) reaction radius, R_{eff}.

Direct Kinetics. Attachment rates for oF_1 and oF_2 were obtained by observing the decay of e_s^- in the near-IR; for all longer oF's and pF's, the strong absorptions of the anions precluded this, so the rates were obtained only from growths of the anions. Growth kinetics of $pF^{-\bullet}$ or $oF^{-\bullet}$ were observed at the strong ($\varepsilon = 70\,000$ M^{-1} cm^{-1} at 580−600 nm)[29] band of $pF^{-\bullet}$ or the nearly identical bands in $oF^{-\bullet}$ having four or more repeat units.

It was necessary to account for kinetics of e_s^-, which undergoes decay with counterions. This decay was measured in neat THF and was accounted for in mechanism in Scheme 1. Ionization of the THF (RH) is followed by solvation of the electron and fragmentation[45] of the THF radical cation, $RH^{+\bullet}$, in $<$1 ps.[39] These processes, [i] and [ii], occur faster than our

SCHEME 1: Reactions in Pulse Radiolysis of THF

$RH \rightarrow RH^{+\bullet} + e_s^-$	(ionization, solvation)		[i]
$RH^{+\bullet} + RH \rightarrow R^\bullet + RH_2^+$	(proton transfer)		[ii]
$e_s^- + pF \rightarrow pF^{-\bullet}$	(e^- attachment)	k_1^{att}	[1]
$e_s^- + AX \rightarrow AX^{-\bullet} \rightarrow A^\bullet + X^\bullet$	(e^- attachment)	k_2^{att}	[2]
$pF^{-\bullet} + RH_2^+, R^\bullet \rightarrow$ products		k_3	[3]
$e_s^- + RH_2^+, R^\bullet, I \rightarrow$ products		k_4	[4]

observations and are treated as occurring instantaneously. The kinetic model thus describes evolution from an initial condition in which e_s^-, solvent radicals ($R^\bullet$), and solvated protons (RH_2^+) are formed at $t = 0$ and evolve with rates $k_1 - k_4$. The competition method, described below, also uses a competitor, AX.

In reaction 4, decay of e_s^- occurs by both geminate and homogeneous reactions[46−49] with the solvated proton and at long times also because of impurities (I) in the solvent not removed by the distillation. The geminate decay with e_s^- thermalized within the Onsager distance[50] of RH_2^+ ions is rapid. The geminate nature means it is first order in concentration but not necessarily exponential in time. A good description of the observed geminate kinetics of e_s^- is obtained by the sum of two exponentials. The homogeneous fraction, having a lifetime of ~0.5 μs depending on purity of the solvent, is represented by a third exponential. Values of these three k_4's determined in neat THF were held fixed during determination of the electron attachment rate, k_1^{att}. Reported attachment rates represent the average of measured rate constants for multiple low concentrations for each pF length. In these direct determinations, reaction 2 in Scheme 1 was absent. Examples of data and fits giving k_1^{att} from growth kinetics are given in Figure 3.

Indirect Observation by Competition. Rates of electron attachment were also determined by competition for electrons with solutes having readily determined rates of reaction with e_s^-. The competition method measured the yield of $pF^{-\bullet}$ or $oF^{-\bullet}$ as a function of the concentration of a competing electron

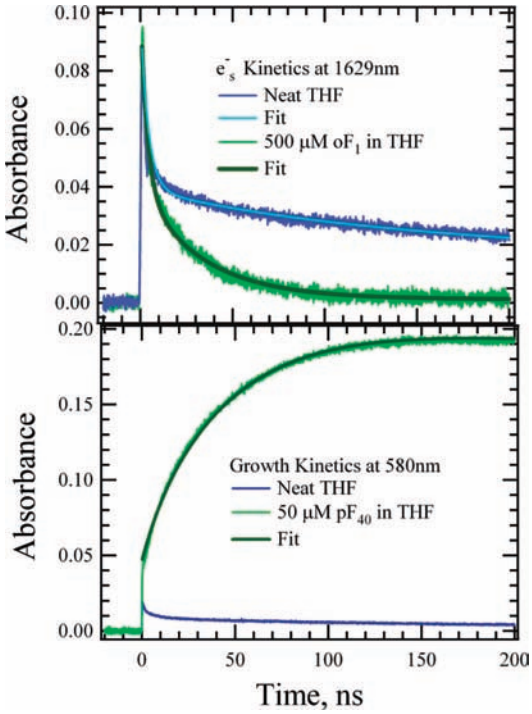

Figure 3. Determination of attachment rates by direct observation of changes in e_s^- decay in the presence of oF_1 (top) and rate of growth of $pF_{40}^{-\bullet}$ (bottom).

TABLE 3: Attachment Rates of Competitors Used in the Indirect Determination of pF Electron Capture Rates along with That for Biphenyl for Comparison[a]

competitor	k^{att} (M^{-1} s^{-1})	R_{eff} (nm)	$t^{1.5}$ (ns)	$t^{1.1}$ (ns)
dibromomethane (DBM)	$8.1 \pm 0.3 \times 10^{10}$	0.82	0.066	1.66
1-iodobutane (BuI)	$7.2 \pm 0.3 \times 10^{10}$	0.73	0.052	1.31
dichloroethane (DCE)	$2.6 \pm 0.4 \times 10^{10}$	0.26	0.007	0.17
biphenyl[b]	$6.4 \pm 0.2 \times 10^{10}$			
biphenyl[c]	$6.4 \pm 0.7 \times 10^{10}$			

[a] These values were determined by observation of e_s^- decay, except where noted, using sufficiently low concentrations to give the long time limiting rate constant, k_{inf}. Also shown are effective reaction distances calculated with eq 2 and times at which the transient term in eq 1 increases the rate by factors of 1.5 and 1.1 relative to k_{inf}. [b] Determined by direct observation of electron decay. [c] Determined by competition with DCE, six concentrations from 0.3 to 4.0 mM.

acceptor. Alkyl halides, AX = 1,2-dichloroethane (DCE), dibromomethane (DBM), or 1-iodobutane (BuI), were especially useful because their radical anions dissociate promptly (<1 ps) to produce products having no optical absorption in the visible. Rate constants for reaction of e_s^- with these competitors, shown in Table 3, were determined by observation of e_s^- decay in a series of AX concentrations. Those rate constants (e_s^- + AX) were not observed to vary significantly with time or concentration as illustrated in Figure S2 in Supporting Information. For most competition experiments, the concentrations of competitors used were low enough that the capture times were slower than the times, shown in Table 3, where the attachment rate constant begins to increase significantly because of the transient term in eq 1. Table 3 also reports the measured rates of electron attachment to biphenyl molecule in THF. Renou et al.[51] reports this rate constant to be $3.9 \pm 0.1 \times 10^{10}$ revising downward the early value[40] of $1.1 \pm 0.3 \times 10^{11}$; Saeki et al.'s[49] value, $5.8 \pm 0.3 \times 10^{10}$, falls between these. The present measurements at low concentrations give $k_{inf} = 6.4 \times 10^{10}$ M^{-1} s^{-1} both by direct electron decay and by the competition method consistent with these previous values. The value for oF_1 is also very close to this.

Rate constants were determined using Scheme 1 now including reaction of e_s^- with AX with rate constant k_2^{att}. Absorbance of $pF^{-\bullet}$ or $oF^{-\bullet}$ ions was measured at times > 0.5 μs, where it was assumed that only homogeneous ions remained. Under those conditions, competition between electron attachment to pF (or oF) with AX as well as decay with radiolysis products of the solvent (k_4) yields a familiar expression for competitive reactions (3) and a corollary (4) that are useful in analyzing such data.

$$[pF^{-\bullet}]/[e_{s,0}^-] = k_1^{att}[pF]/(k_1^{att}[pF] + k_2^{att}[AX] + k_4) \quad (3)$$

$$k_1^{att}[pF] = R \times k_1^{att}[AX]/(1 - R) - k_4 \quad (4)$$

In eq 3, $[e_{s,0}^-]$ is the concentration of solvated electrons in the absence of all three decay processes. The ratio R in eq 4 is defined below. Figure 4 shows typical competition data used to determine the rate constant for electron attachment, in this example, to a 133 unit long pF.

Figure 4a displays absorbance due to pF anions in a solution containing pF alone or with varied concentrations of AX = DCE. Each trace is divided by the trace with pF alone in the "ratio plot", Figure 4b, to give the ratio $R = [pF^{-\bullet}]_{[AX]}/[pF^{-\bullet}]$ as a function of time. The lines in the ratio plot become nearly flat when capture of e_s^- is complete except for fluctuations because of lamp irreproducibility. This flatness indicates that while e_s^- reacts rapidly with AX, $pF^{-\bullet}$ (or $oF^{-\bullet}$) does not. The

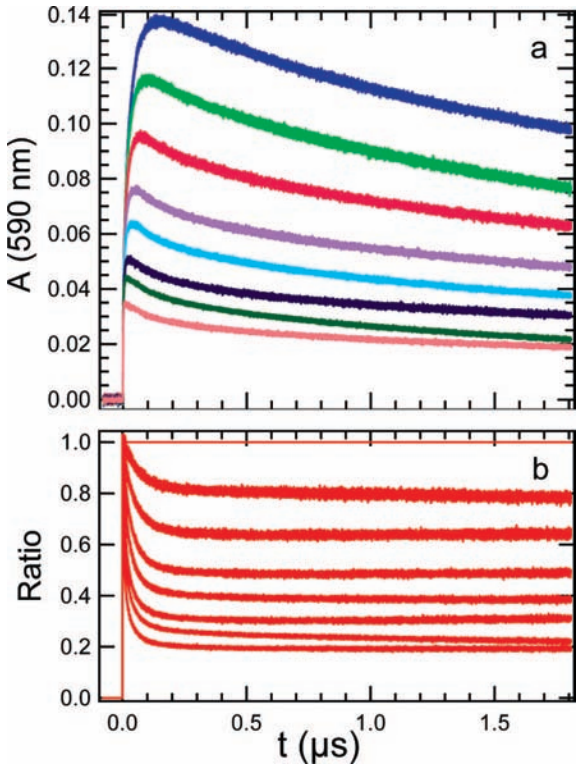

Figure 4. Growth and decay of $pF^{-\bullet}$ at 590 nm as pF_{133} captures e_s^-. (a) $pF^{-\bullet}$ absorbance for 20.4 μM pF_{133} (polymer molecule concentration) in THF alone (top trace, blue) or with DCE as a competitor; [DCE] = 0.33, 0.66, 1.32, 1.98, 3.28, 4.9, and 8.11 mM. (b) A "ratio plot" in which each trace in (a) is divided by the top trace (without DCE). From these ratios, eq 4 gives the rate constant k_1^{att} for electron capture by pF_{133}.

flat ratio plots also inform us that the decay rate of $pF^{-\bullet}$ (or $oF^{-\bullet}$) (k_3) is not affected when competition by AX removes large fractions of electrons. The constant values of $R(t)$ in the flat region were used along with values for k_2^{att} (Table 3) in eq 4 to obtain the rate for electron capture by pF. The rate constants for electron attachment, k_1^{att}, at low concentrations of different length oF's and pF's obtained in this way are included in Table 2 and Figure 2. At comparable concentrations to those used in Figure 4, DBM and BuI competitors also give similar "flat" ratio plots. As the concentration of the competitor (e.g., DBM) increases, oF or pF captures electrons within a shorter time window. The shortest times were reached with concentrations of up to 800 mM of DBM. At such high concentrations, the added DBM did cause noticeable decay of $pF^{-\bullet}$, so the ratio plots were not flat because of either a slow reaction of $pF^{-\bullet}$ with DBM or an impurity. In those cases, the decay was extrapolated to $t = 0$. The resulting yield [$pF^{-\bullet}$] at $t = 0$ was reduced by 30% to estimate the homogeneous yield (see below).

Corrections were made for small absorptions due to pF cations and triplets. Yields of cations are small in THF because of the rapid fragmentation reaction ii. For 20 μM pF in THF observed at 590 nm, about 1.6% of the absorption was due to cations, $pF^{+\bullet}$, probably formed by direct ionization. About 1.2% of the signal was due to pF triplets likely formed by a combination of direct energy deposition and Cerenkov reabsorption. The absorption band[29] of $pF^{+\bullet}$ is nearly identical to that of $pF^{-\bullet}$; the triplet maximum is at 760 nm but contributes also at 590 nm. These contributions were measured in separate experiments with and without DCE or DBM as well as added O_2, which reacts with $pF^{-\bullet}$ and pF triplets. These contributions were subtracted prior to determination of rates using eqs 3 and 4. The competiton results may be affected by "dry" electron capture by the pF's or by the competitors. These were minimized by use of low concentrations. These effects are noted in the discussion section.

The competition data also provide information about the decay kinetics of $pF^{-\bullet}$ (or $oF^{-\bullet}$). At low to moderate concentrations of pF, the earlier portions of $pF^{-\bullet}$ decay are not readily observed because $pF^{-\bullet}$ growth occurs on the same time scale. See, for example, the uppermost trace in Figure 4a. As a result, neither the rate process for electron attachment, k_1^{att}, nor the geminate decay rate can be well characterized. If the kinetic form of either the growth or decay were definitively known, for example, if $pF^{-\bullet}$ growth were a simple pseudo-first-order reaction (single exponential), then both the growth and decay could be determined from data such as that in Figure 4a at a series of concentrations. However, the growth of $pF^{-\bullet}$ is not known; one of the goals of this paper is to determine how well it follows the time dependence predicted by eq 1 especially for long pF's having large effective capture radii, R_{eff}. Competition by AX reduces the lifetime of e_s^- so that $pF^{-\bullet}$ growth stops at an early time revealing the $pF^{-\bullet}$ decay kinetics except at the shortest times. For example, from the lower four traces in Figure 4, 30% of the $pF^{-\bullet}$ ions decay more rapidly (~100 ns), probably because of geminate recombination, although that component was not readily discernible in the first trace for which [DCE] = 0. Knowledge of the decay kinetics then enabled more accurate determination of k_1^{att} from direct observation of $pF^{-\bullet}$ growth and was used in the fitting of such data in the previous section as well as data from competition experiments at high concentrations described in section 2.

k_{inf} as a Function of Length. The experimental results enable determination of how k_{inf} and therefore R_{eff} depend on length. Table 2 shows that rate constants, k_{inf}, for attachment of electrons to oF or pF (denoted collectively as pF) increase from 5.8×10^{10} for oF_1 to 1.1×10^{12} M^{-1} s^{-1} for pF_{133}. This increase by a factor of 16 is much smaller than the 133-fold increase in length as expected for diffusion-controlled reactions with long molecules. It shows the strong influence of "diffusive interaction (DI)".[3,4,16,23,52] If pF_{133} is regarded as 133 reactive sites spaced along a line, reaction of an electron with one of them removes that electron precluding reaction of that electron with any of the other sites. Data in Figure 2 indicates that DI reduced the rate by a factor of 133/16 = 8.3. Even with the effect of DI, the rate constants k_{inf} for long pF's are still large at ~10^{12} M^{-1} s^{-1}. For these high rate constants, R_{eff} exceeds 10 nm. Equation 1 would therefore predict a large transient term observable at higher concentrations of polymer.

Theoretical models describing diffusion-controlled reactions of nonspherical molecules discussed below are pictured in Figure 5.

Prolate Spheroid. The experimental measurements in Figure 2 are described well with eq 2 and R_{eff} calculated by modeling the polymer chain as a prolate spheroid of length L and reaction radius r_x, which defines the half-width at the center or semiminor axis length:[5]

$$R_{eff} = L \times z/(\ln((1+z)/(1-z))) \quad z = (1 - (2r_x/L)^2)^{1/2} \tag{5}$$

Touching Spheres. For a straight line of N touching spheres of radius r_x, Traytak[3] gave an asymptotic expression. Later, Tsao et al. gave eq 6, which is accurate to higher orders and was tested up to N_{sp}= 100 spheres by Monte-Carlo methods:[4]

$$R_{eff} = r_x N/(\ln(N_{sp}) + a + b/N_{sp}) \quad a = 0.438, b = 0.611 \tag{6}$$

Because this solution[3,4] is for touching spheres, the number of spheres used is determined by L and r_x. N_{sp} is not the

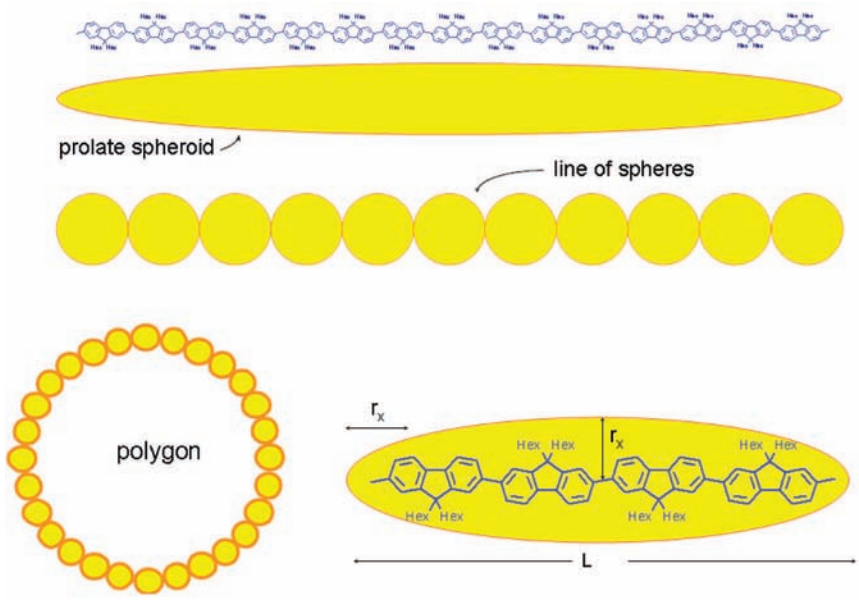

Figure 5. A 15 unit oligomer, pF_{15}, and its representation as a prolate spheroid or as touching spheres in a line. Shown at a reduced scale is a polygon (circle) that would represent a longer polymer. Solutions have been reported for diffusion-controlled reaction with each of these objects. The sketch at the lower right depicts a prolate spheroid at larger magnification for an F_4 oligomer showing the length, L, and reaction radius, r_x, which defines the half-width (semiminor axis) of the spheroid; r_x is also the radius of each of the spheres in the line and polygon.

number of repeat units in the polymer but is given by $N_{sp} = 1 + L/2r_x$. For pF_{133} and $r_x = 0.63$ nm, 88 spheres were used. Equation 6 similarly describes diffusion-controlled reactions with spheres arrayed in a circular hollow polygon using $a = 1.07$ and $b = -1.10$.

Cylinders. The flux to a cylinder has been used to discuss reactions of $OH^•$ radicals with DNA assuming constant production of $OH^•$ radicals at a finite distance from DNA.[53] A steady-state solution can be obtained only by assuming that constant concentration is reached at a fixed distance from the molecule. This assumption is not as appropriate in the current work, so the cylindrical model is not utilized here.

Comparison of Models. The data in Figure 2 were well described by the model describing the polymer molecule as a prolate spheroid. The fit shown there was obtained by substituting R_{eff} given by eq 5 into eq 2. The best fit gave a reaction distance $r_x = 0.63$ nm. This reaction distance is just slightly larger than the value of R_{eff} for oF_1 (Table 2). The agreement of these values supports the notion that these reactions are diffusion-controlled. Figure 6 compares the predictions of the prolate spheroid model with other models. The values of R_{eff}, and therefore rate constants, for a linear chain of touching spheres are almost identical to those of the prolate spheroid model; both models provide good descriptions of the data. An advantage of the prolate spheroid model is that it does not require approximations. An advantage of the line of spheres is that it does not narrow toward its ends as does the spheroid. That difference is probably responsible for the slightly smaller flux (smaller R_{eff}) to the prolate spheroid seen in Figure 6, where both have the same width at their centers. The reason the difference between the two models is small is the weak dependence on the width, r_x. For example, eq 5 predicts that a factor of 2 change in r_x produces only a 10−20% change in R_{eff} for lengths between 100 and 5 nm.

Attachment rates may also yield information about the conformation of the polymers. The results show substantial increases of rate with length that are well accounted for by calculations of diffusion-controlled reaction with long, rigid rods.

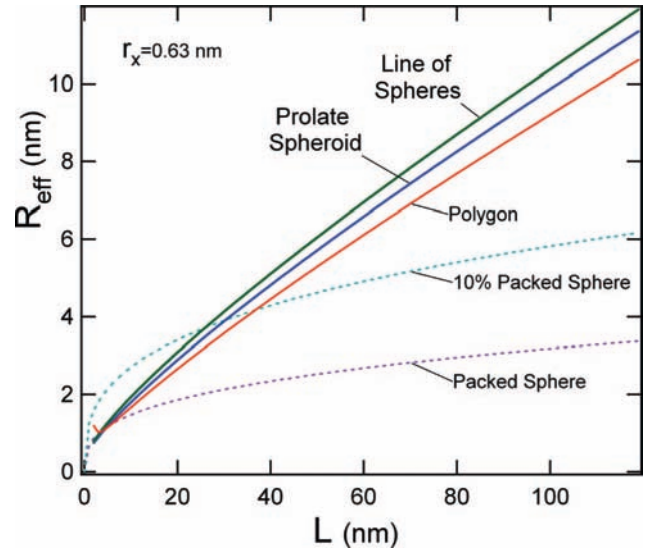

Figure 6. Comparison of models for computing long time rate constants for diffusion-controlled reactions with conjugated polymers given as the effective reaction radius R_{eff}. The prolate spheroid fit to the data in Figure 2 is compared to arrays of spheres of the same radius, r_x, arranged along a line[3,4] and on a regular polygon[3,4] or a packed sphere. Also shown is diffusion-controlled attachment to a sphere in which the density of reactive sites is 10% giving a larger R_{eff} for the same amount of reactive material.

Implications of the results for the conformations of pF molecules in solution will be discussed in the next section.

The dependence of k_{inf} on the length of the molecule, shown in Figure 2, is noticeably nonlinear at short lengths. At long lengths ($n > 50$), it becomes almost linear. At those long lengths, each additional monomer unit increases k_{inf} by an almost constant increment of 6.4×10^9 M^{-1} s^{-1}: the rate of electron capture per repeat unit is one decade smaller than that for a single unit, F_1, so k_{inf} is approximately linear but with a much reduced value because of diffusive interaction. The nonlinearity to reach this lower value is largest at the beginning: k_{inf} to two

touching spheres is not double that to one sphere but is larger by only a factor of 1.38.[54]

Information about Polymer Conformation from Diffusion-Controlled Reactions. Data in Figures 2 and 6 showed that the dependence of k_{inf} on length is well described by either the prolate sphereoid or line of spheres models; both treat the polymer as straight rigid rods, although a wealth of data on conjugated polymers shows that they can curve, coil, and in some cases even collapse into relatively compact globular structures.[55−57] On the basis of light-scattering results, Grell et al.[58] found that polyoctylfluorenes in THF, while relatively stiff polymers, could be characterized by a Kuhn length of 17 nm or about 20 polymer repeat units indicating curvature over this length. Grell et al. noted that this is expected because of the 19° angle between adjacent 0.836 nm long repeat units. If significant numbers of these bends in the backbone of the chain are in a similar direction, it is possible to conceive structures for the longer pFs where the polymers can curve back on themselves to form less open structures. On the basis of the 19° angle, such circular structures, although improbable, would at least be possible for chains of as few as 20 repeat units.

Figure 6 shows that in addition to the straight rod models the polygon model is also compatible with the data in Figure 2. This model computes diffusion to touching spheres arrayed on vertices of a planar polygon, effectively a circle. The similarity of this model to that of straight rod of the same length indicates that the rate of diffusion-controlled reaction is not sensitive to moderate curvature. On the other hand, the data are not compatible with models of "collapsed" polymers on the basis of spheres, squares, or cubes as noted earlier for hole capture by PPV.[27] Of special interest is the partially filled sphere in which the reactive units (those spheres distributed along a line, polygon, etc.) are confined within a larger sphere but at a density less than close packed. Such a sphere filled with 90% solvent and 10% polymer would have a radius 2.15 times ($10^{1/3}$) larger than the radius, R_{cp}, of a closely packed sphere filled entirely with the polymer. Deutsch et al.[16] found that the diffusion-controlled flux to such a low-density sphere falls slowly with decreasing density being 90% as large as a closely packed sphere of the same size. Because of connectivity of the polymers, this model provides an overestimate of the diffusion-controlled capture by a polymer coiled into a spherical volume. The model of a 10% sphere having $R_{eff} = 0.9 \times 2.15 \times R_{cp}$ is not compatible with the data. From these comparisons, we can conclude that the pF's, while likely curved, are effectively still very extended structures. In particular, structures that are compressed because of attractive forces between chains appear to be unlikely for these pF's in THF.

2. The Transient Term and Time-Dependent Rate Coefficients. Once R_{eff} is determined, eq 1 makes definite predictions about the time dependence of the electron capture rate that can be compared with the measurements. While the transient term in eq 1 was first described in 1917, its first observation came in 1975.[8,59,60] The early papers and several subsequent ones[11,24−26] employed direct measurement of decay kinetics, especially of fluorescence, or sometimes of growth kinetics, to evaluate the time dependence of $k(t)$. In the present work, $pF^{-\bullet}$ growth kinetics can provide such information, but extraction of the nonexponential contributions is inherently uncertain particularly in the presence of geminate and homogeneous decay that masks the actual growth or decay kinetics. An alternative is to determine pseudo-first-order time-dependent rate constants at a series of concentrations.[9,59−61] The simplest implementation utilizes the competition method described above determining

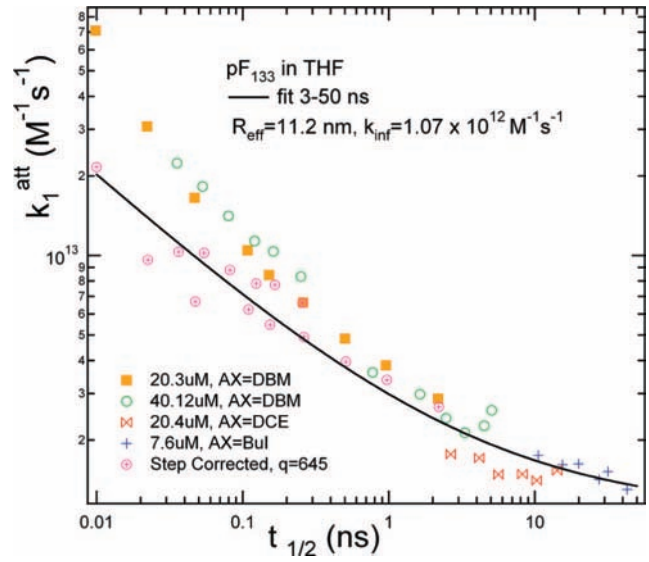

Figure 7. Rate constants for electron capture by pF_{133} as a function of time from competition experiments in which the average capture time, $t_{1/2}$, is shortened by increasing the concentration of the competitor. The solid line is the prediction of eq 1 using $D = D(e_s^-) + D(pF_{133}) = 1.255 \times 10^{-4}$ cm^2/s.[1,2] The different markers indicate series of experiments having differing pF concentration and competitor concentrations noted in the legend at the lower left. Inclusion of fast "step" electron capture is discussed below.

$k_1^{att}(t)$ utilizing eqs 3 and 4. In contrast to experiments described above, AX will not be kept small but will be increased to make the average lifetime of solvated electrons progressively shorter. For a given concentration of AX, the average (median) time over which electrons are captured by pF is given by the first half-life of e_s^- as it decays by all three processes in Scheme 1:

$$t_{1/2} = \ln(2)/(k_1^{att}[pF] + k_2^{att}[AX] + k_4) \quad (7)$$

Figure 7 shows the time dependence of $k_1^{att}(t)$ for electron capture by pF_{133} determined using eq 3 with t defined by eq 7. The extraction of $k(t)$ and $t = t_{1/2}$ from the competition data is simple and direct, and they yield an appealing, visual test of the time dependence predicted by eq 1, but they employ approximations analyzed in the next section. Indeed, Figure 7 shows that eq 1 describes the time dependence extracted in this fashion only approximately. Because the approximations are best at long times, the fit shown was determined using only lower concentration data giving half-lives in the range of 3−50 ns. The fit curve was then extended to shorter times as shown producing an apparent large departure from prediction of the time-dependent Schmoluchowski equation, which will be addressed with a more exact method later.

Figure 8 shows similar data for two different oligomers, oF_1 and oF_6. For the six-unit oligomer, the data departs from the predictions of eq 1 as did the data for pF_{133}. On the other hand, eq 1 unsurprisingly provides an adequate description of the rates of electron capture over all times tested for oF_1, which is a small nearly spherical molecule. The fitted k_{inf} from competition experiments is in excellent agreement with the attachment rate to biphenyl in THF determined here and that reported by Saeki et al.[49]

Analysis of Apparent Deviations from the Modified Schmoluckowski Equation, Eq 1. In this section, we improve upon the approximations used in obtaining $k_1^{att}(t)$ in Figures 7 and 8. The data have been compared with the predictions of eq 1 in which the only parameters are k_{inf} (or R_{eff}), determined from low concentration data, and D, which is known independently.

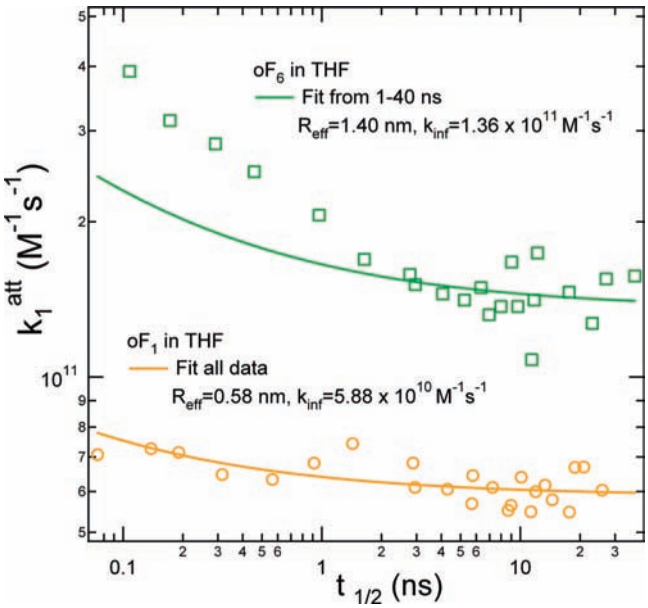

Figure 8. Time dependence of electron capture by oF_1 (400, 800, and 3840 μM) and oF_6 (100, 400, and 970 μM) oligomers in THF determined by competition with DCE. Larger oligomer concentrations were used to access shorter times.

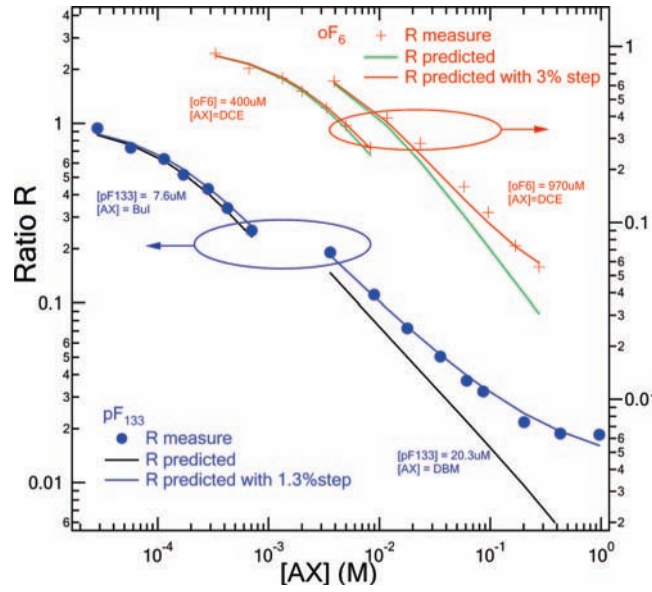

Figure 9. Comparison of the measured ratios $pF^{-\bullet}([AX])/pF^{-\bullet}([AX] = 0)$ to ratios predicted by eqs 8 and 9. The concentration dependence of these ratios assesses the time-dependent form of electron attachment rate given by eq 1. For pF_{133}, good fits to both competitor sets ([pF] = 7.6 μM for BuI and 20.3 μM for DBM) were obtained using the same common parameters of $R_{eff} = 11.37$ nm, $k_{inf} = 1.08 \times 10^{12}$ M^{-1} s^{-1}, and $D = 1.3 \times 10^{-4}$ cm^2 s^{-1}. For the seven measurements on the left of the graph, the lower concentration (7.6 μM) of pF was used to more accurately measure the rate at long times. The two sets of data are not expected to meet but to display a vertical offset by a factor somewhat smaller than the ratio of pF concentrations. The actual offsets agree with those expected on the basis of the (20.3/7.6) ratio of concentrations. Similarly, for oF_6, $R_{eff} = 1.2$ nm and $k_{inf} = 1.23 \times 10^{11}$ M^{-1} s^{-1}.

The comparison suggests that the experimental increase in $k(t)$ at short times is larger than that expected by eq 1 as depicted in Figures 7 and 8.

On the basis of the experimental value of $R_{eff} = 11.37$ nm for pF_{133}, eq 1 predicts $k_1^{att}(t)$ to increase by more than a factor of 10 from its k_{inf} value at times as short as 0.1 ns. Utilizing eqs 3 and 4, the measurements in Figure 7 find a larger increase. However, eqs 3 and 4 are approximate as they treat $k_1^{att}(t)$ as constant over the lifetime of the electrons for a given concentration of the competitor. The rate constant $k_2^{att}(t)$ for electron capture by the competitor, AX, is similarly treated as constant, using the low concentration values in Table 3. While still inexact, this is a better approximation because AX is a small molecule leading to less time dependence. We correct these approximations here by explicitly including the time dependence for attachment to both the polymer and the competitor using values of R_{eff} for the competitors given in Table 3. If the time-dependent form of the electron attachment rates $k_1^{att}(t)$ and $k_2^{att}(t)$ can be assumed to be of that given by eq 1, a set of rate equations describing $[pF^{-\bullet}]$ as a function of [AX] can be analytically integrated (see Supporting Information for details) resulting in a total yield of $[pF^{-\bullet}]$ as a function of R_{eff} (or k_{inf}) and [AX]:

$$[pF^{-\cdot}]_{[AX]} = \frac{1}{a} + \left[\frac{R_{eff,pF}}{\sqrt{Da}} - \frac{b\sqrt{\pi}}{2a^{3/2}}\right]\mathrm{erfc}\left(\frac{b}{2\sqrt{a}}\right)\exp(b^2/4a) \tag{8}$$

$$a = 4\pi N_A D(R_{eff,pF}[pF]_0 + R_{eff,AX}[AX]_0) + k_4$$
$$b = 8N_A\sqrt{\pi D}([pF]_0 R_{eff,pF}^2 + [AX]_0 R_{eff,AX}^2) \tag{9}$$
$$R_{predict} = [pF^{-\cdot}]_{[AX]}/[pF^{-\cdot}]_{[AX]=0}$$

Equations 8 and 9 can then predict the ratios of $pF^{-\bullet}$ formed with and without competition of electron capture by AX. Comparison of these predicted values with the experimentally determined ratio values ($R_{measure}$) is displayed in Figure 9.

It can be seen that for [AX] concentrations less than 10−100 mM, where the average (median) time of electron capture is greater than 1 ns, excellent agreement between $R_{predict}$ and $R_{measure}$ is observed shown by the black and green curves for pF_{133} and oF_6, respectively. This agreement means that eq 1 gives an excellent description of $k_1^{att}(t)$ for $t_{1/2} > 1$ ns.

At the highest [AX], where electron attachment occurs in a very short time window, the predicted curves deviate from the experimental points in Figure 9. This observation that the experimentally determined ratios are higher than the predicted ones could signal a larger increase in $k(t)$ than predicted by eq 1. Such a result would be unexpected because the transient term in eq 1 is already an upper bound of the asymptotic series solution to the modified Smoluchowski equation for diffusive interaction of spherical reactants.[62,63] Rather, the larger ratio and thus higher yield of $pF^{-\bullet}$ at short times in the presence of AX likely indicates that electron attachment to the pF may not be solely due to diffusive motions of reactants, e_s^- and pF, finding each other. Alternatively, some $pF^{-\bullet}$ may be formed in ultrafast "step" processes by reactions of precursors of e_s^-. This phenomenon is well-known for hot electrons introduced by pulse radiolysis, where presolvated or "dry" electrons are captured rapidly, before solvation in water and alcohols,[64−66] and has recently been reported for electron attachment to biphenyl in THF.[49] One conceivable mechanism for such prompt capture is attachment of highly mobile nonthermalized electrons to the molecules. The difference between observation and prediction in Figure 9 would be accommodated if the 20.3 μM pF_{133} captured ∼ 1.3% of electrons prior to solvation as shown in Figure 9 (blue and red curves). A larger amount would be required if the competitor (e.g., DBM) also captures electrons prior to solvation. In terms of the expression[64−66] $1 - \exp(-q \times c)$ for the fraction of electrons captured before solvation, capture of 1.3% prior to solvation corresponds to $q = 645$ M^{-1}

for $c = 20.3$ μM of polymer or $q = 4.8$ on a repeat unit concentration basis. For oF_6, 3% capture corresponds to a similar value, $q = 5.3$ per repeat. The similar electron capture per repeat unit implies a similar mechanism. Figure 7 also displays rate constants obtained if this presolvation electron capture is taken into account. At low competitor concentrations, most electrons are electrons captured by pF so the effect of this small amount of presolvation capture is expected and is hardly noticeable. The excellent agreement over all concentrations in Figure 9 supports the conclusion that the simple form of eq 1 provides a good description of the experimental observations. For the longest polymer, pF_{133}, the electron capture rate coefficient is well described by the solid line in Figure 7 increasing, at short times, by more than a decade over the steady-state value.

Such a large increase in $k(t)$ means that the transient term is dominant at short times signaling a different dependence of the rate on R_{eff}. Equation 1 can be written as $k(t) = 4\pi DN_A(R_{eff} + R_{eff}^2/(\pi Dt)^{1/2})$. The rates determined here have entered a regime where $k(t)$ is approximately proportional to R_{eff}^2.

While the intuitive extraction of $k(t)$ in Figure 7 is less precise, it leads to the same conclusion: rate coefficients have a strong dependence on time that is in reasonable accord with eq 1. The accord is very good to excellent if a small amount of presolvation electron capture is taken into account.

An additional, though unexceptional, mechanism for prompt capture[67,68] should be taken into account. If electrons are initially localized on or near (within r_x) a pF molecule, they would likely be captured promptly. This mechanism with $r_x = 0.63$ nm can account for only a tenth of the 1.3% of prompt capture suggested by the data of Figure 9. Consequently, it is reasonable to attribute most of the prompt capture to presolvated electrons. Additional preliminary observations at higher concentrations in this laboratory support this assignment. In the future, we hope these will enable a quantitative assessment of the accuracy of eq 1 to times near 10^{-11} s.

Related Observations for Reaction of OH• radicals with DNA. Reactions of OH• radicals with varied forms of DNA have received attention[53,67,69−71] because the effects of radiation on living cells including cell death and mutations are thought to arise principally from damage to DNA resulting from OH• attack. The largest rate constants were 10^9-10^{10} M^{-1} s^{-1} (per residue concentration) found for the SV40 minichromosome having 10 486 residues (bases). The rate constants were determined by competition measuring the yields of DNA strand breaks, which are due to OH• attack. This corresponds to rate constants for OH• reaction with the entire assembly of $10^{13}-10^{14}$ M^{-1} s^{-1}. Somewhat slower values were reported for other DNAs. These reactions have been discussed in terms of a cylindrical model. The SV40 minichromosome coils into 22 nucleosomes, each 11 nm in diameter and 6 nm long, but with thinner (~2 nm × 30 nm long) segments between the nucleosomes that also react with OH•. The actual conformations and dimensions may be less well-known in solution than in cells, but the overall length could be as large as 792 nm, which is substantially longer than the molecules studied here. For a 792 nm length, eq 5 with average radii of 2−4 nm gives rate constants $k_{inf} = 1.4-1.6 \times 10^{12}$ M^{-1} s^{-1}, which is slower than the observed values.[69] However, this discrepancy may be due to the time dependence. Taking the average radius to be 3 nm and $D = D(OH^•) = 2.8 \times 10^{-5}$ cm^2/s,[72] application of eq 1 to include the time dependence predicts $k(t)$ from $1.9-22 \times 10^{13}$ M^{-1} s^{-1} in reasonable accord with the observations of Ly et al.[69] for their observation times from 500 to 3 ns. Equation 1 predicts that for this very long molecule $k(t)$ will approach k_{inf} (within 10%) only for times of ~50 ms.

Conclusions

Diffusion-controlled rate constants having long time limits, k_{inf}, as large as 10^{12} M^{-1} s^{-1}, corresponding to effective reaction radii, R_{eff}, as large as 11.4 nm, were found for diffusion-controlled reactions of solvated electrons with oligo and polyfluorene molecules in solution. Theories that compute the increase of R_{eff} and k_{inf} with length of the molecule predicted well the observed increase of k_{inf}. Large transient effects were observed in which $k(t)$ increases by more than a decade at early times for longer molecules. These transient effects were anticipated by theory;[27−29,73] the present results support these theories. The size of the transient terms and the quantitative confirmation of eq 1 are unprecedented. As predicted, these transient effects are largest and persist to longer times when R_{eff} is large. Predictions of transient behavior by eq 1 are verified to ~0.1 ns where $k(t)$ has increased by almost a factor of 10 over k_{inf}. At shorter times (higher competitor concentrations), deviations occur. While the deviations could signal errors in eq 1, an alternative explanation of prompt capture of electrons before solvation is likely and is in quantitative agreement with the observations.

Acknowledgment. This work was supported by the U.S. Department of Energy, Office of Basic Energy Sciences, Division of Chemical Sciences, under contract DE-AC02-98-CH10886.

Supporting Information Available: The derivation of eqs 8 and 9, an illustration of their use, and rate constants for electron capture by alkyl halides used herein as a function of concentration. This material is available free of charge via the Internet at http://pubs.acs.org.

References and Notes

(1) Heimlich, Y.; Rozenshtein, V.; Levanon, H.; Lukin, L. *J. Phys. Chem. A* **1999**, *103*, 2917–2924.
(2) Dodelet, J. P.; Freeman, G. R. *Can. J. Chem.-Rev. Can. Chim.* **1975**, *53*, 1263–1274.
(3) Traytak, S. D. *Chem. Phys. Lett.* **1992**, *197*, 247–254.
(4) Tsao, H. K.; Lu, S. Y.; Tseng, C. Y. *J. Chem. Phys.* **2001**, *115*, 3827–3833.
(5) Richter, P. H.; Eigen, M. *Biophys. Chem.* **1974**, *2*, 255–263.
(6) Smoluchowski, M. *Z. Phys. Chem.* **1917**, *92*, 167.
(7) Collins, F. C.; Kimball, G. E. *J. Colloid Sci.* **1949**, *4*, 425–37.
(8) Nemzek, T. L.; Ware, W. R. *J. Chem. Phys.* **1975**, *62*, 477–489.
(9) Noyes, R. M. *Prog. React. Kinet. Mech.* **1961**, *1*, 129–160.
(10) Keizer, J. *Chem. Rev.* **1987**, *87*, 167–180.
(11) Sikorski, M.; Krystkowiak, E.; Steer, R. P. *J. Photochem. Photobiol., A: Chem.* **1998**, *117*, 1–16.
(12) Pilling, M. J.; Rice, S. A. *J. Chem. Soc., Faraday Trans. 2* **1975**, *71*, 1563–1571.
(13) Rice, S. A.; Pilling, M. J. *Prog. React. Kinet.* **1978**, *9*, 93–194.
(14) Litniewski, M.; Gorecki, J. *J. Chem. Phys.* **2005**, 122.
(15) Gosele, U.; Hauser, M.; Klein, U. K. A.; Frey, R. *Chem. Phys. Lett.* **1975**, *34*, 519–522.
(16) Deutch, J. M.; Felderhof, B. U.; Saxton, M. J. *J. Chem. Phys.* **1976**, *64*, 4559–4563.
(17) Cukier, R. I. *J. Stat. Phys.* **1983**, *30*, 383–389.
(18) Cukier, R. I. *J. Stat. Phys.* **1986**, *42*, 69–82.
(19) Tokuyama, M.; Cukier, R. I. *J. Chem. Phys.* **1982**, *76*, 6202–6214.
(20) Traytak, S. D. *Chem. Phys. Lett.* **1994**, *227*, 180–186.
(21) Traytak, S. D. *Physica A: Stat. Mech. Appl.* **2006**, *362*, 240–248.
(22) Tseng, C. Y.; Tsao, H. K. *J. Chem. Phys.* **2002**, *117*, 3448–3453.
(23) Chekunaev, N. I. *Chem. Phys.* **2004**, *300*, 253–266.
(24) Andre, J. C.; Niclause, M.; Ware, W. R. *Chem. Phys.* **1978**, *28*, 371–377.
(25) Burel, L.; Mostafavi, M.; Murata, S.; Tachiya, M. *J. Phys. Chem. A* **1999**, *103*, 5882–5888.

(26) Allonas, X.; Jacques, P.; Accary, A.; Kessler, M.; Heisel, F. *J. Fluoresc.* **2000**, *10*, 237–245.
(27) Grozema, F. C.; Hoofman, R.; Candeias, L. P.; de Haas, M. P.; Warman, J. M.; Siebbeles, L. D. A. *J. Phys. Chem. A* **2003**, *107*, 5976–5986.
(28) Funston, A. M.; Silverman, E. E.; Miller, J. R.; Schanze, K. S. *J. Phys. Chem. B* **2004**, *108*, 1544–1555.
(29) Takeda, N.; Asaoka, S.; Miller, J. R. *J. Am. Chem. Soc.* **2006**, *128*, 16073–16082.
(30) Pilling, M. J.; Rice, S. A. *J. Chem. Soc., Faraday Trans. 2* **1976**, *72*, 792–801.
(31) Butler, P. R.; Pilling, M. J.; Rice, S. A.; Stone, T. J. *Can. J. Chem.-Rev. Can. Chim.* **1977**, *55*, 2124–2132.
(32) Zhou, H. X.; Szabo, A. *Biophys. J.* **1996**, *71*, 2440–2457.
(33) Geng, Y.; Trajkovska, A.; Katsis, D.; Ou, J. J.; Culligan, S. W.; Chen, S. H. *J. Am. Chem. Soc.* **2002**, *124*, 8337–8347.
(34) Tsolakis, P. K.; Kallitsis, J. K. *Chem.-Eur. J.* **2003**, *9*, 936–943.
(35) Klaerner, G.; Miller, R. D. *Macromolecules* **1998**, *31*, 2007–2009.
(36) Wishart, J. F. In *Radiation Chemistry: Present Status and Future Trends*; Jonah, C. D., Rao, B. S. M., Eds.; Elsevier Science: Amsterdam, 2001; Vol. 87, pp 21−35.
(37) Wishart, J. F.; Cook, A. R.; Miller, J. R. *Rev. Sci. Instrum.* **2004**, *75*, 4359–4366.
(38) Miller, J. R.; Penfield, K.; Johnson, M.; Closs, G.; Green, N. In *Photochemistry and Radiation Chemistry. Complementary Methods for the Study of Electron Transfer*; Wishart, J. F., Nocera, D. G., Eds.; American Chemical Society: Washington D.C., 1998; Vol. 254, p 161−176.
(39) Martini, I. B.; Barthel, E. R.; Schwartz, B. J. *J. Chem. Phys.* **2000**, *113*, 11245–11257.
(40) Bockrath, B.; Dorfman, L. M. *J. Phys. Chem.* **1973**, *77*, 1002–1006.
(41) Somma, E.; Loppinet, B.; Chi, C.; Fytas, G.; Wegner, G. *Phys. Chem. Chem. Phys.* **2006**, *8*, 2773–2778.
(42) Fytas, G.; Nothofer, H. G.; Scherf, U.; Vlassopoulos, D.; Meier, G. *Macromolecules* **2002**, *35*, 481–488.
(43) Pedersen, S. U.; Christensen, T. B.; Thomasen, T.; Daasbjerg, K. *J. Electroanal. Chem.* **1998**, *454*, 123–143.
(44) Amatore, C.; Azzabi, M.; Calas, P.; Jutand, A.; Lefrou, C.; Rollin, Y. *J. Electroanal. Chem.* **1990**, *288*, 45–63.
(45) Tranthi, T. H.; Koulkes-Pujo, A. M. *J. Phys. Chem.* **1983**, *87*, 1166–1169.
(46) Closs, G. L.; Calcaterra, L. T.; Green, N. J.; Penfield, K. W.; Miller, J. R. *J. Phys. Chem.* **1986**, *90*, 3673–3683.
(47) Takeda, N.; Poliakov, P. V.; Cook, A. R.; Miller, J. R. *J. Am. Chem. Soc.* **2004**, *126*, 4301–4309.
(48) De Waele, V.; Sorgues, S.; Pernot, P.; Marignier, J. L.; Monard, H.; Larbre, J. P.; Mostafavi, M. *Chem. Phys. Lett.* **2006**, *423*, 30–34.
(49) Saeki, A.; Kozawa, T.; Ohnishi, Y.; Tagawa, S. *J. Phys. Chem. A* **2007**, *111*, 1229–1235.
(50) Onsager, L. *Phys. Rev.* **1938**, *54*, 554–557.
(51) Renou, F.; Archirel, P.; Pernot, P.; Levy, B.; Mostafavi, M. *J. Phys. Chem. A* **2004**, *108*, 987–995.
(52) Tsao, H. K. *Phys. Rev. E* **2002**, 66.
(53) Udovicic, L.; Mark, F.; Bothe, E.; Schultefrohlinde, D. *Int. J. Radiat. Biol.* **1991**, *59*, 677–697.
(54) Samson, R.; Deutch, J. M. *J. Chem. Phys.* **1977**, *67*, 847–847.
(55) Hu, D. H.; Yu, J.; Wong, K.; Bagchi, B.; Rossky, P. J.; Barbara, P. F. *Nature* **2000**, *405*, 1030–1033.
(56) Grey, J. K.; Kim, D. Y.; Donley, C. L.; Miller, W. L.; Kim, J. S.; Silva, C.; Friend, R. H.; Barbara, P. F. *J. Phys. Chem. B* **2006**, *110*, 18898–18903.
(57) Wong, K. F.; Skaf, M. S.; Yang, C. Y.; Rossky, P. J.; Bagchi, B.; Hu, D. H.; Yu, J.; Barbara, P. F. *J. Phys. Chem. B* **2001**, *105*, 6103–6107.
(58) Grell, M.; Bradley, D. D. C.; Long, X.; Chamberlain, T.; Inbasekaran, M.; Woo, E. P.; Soliman, M. *Acta Polym.* **1998**, *49*, 439–444.
(59) Jonah, C. D.; Miller, J. R.; Hart, E. J.; Matheson, M. S. *J. Phys. Chem.* **1975**, *79*, 2705–2711.
(60) Buxton, G. V.; Cattell, F. C. R.; Dainton, F. S. *J. Chem. Soc., Faraday Trans. 1* **1975**, *71*, 115–122.
(61) Schwarz, H. A. *J. Chem. Phys.* **1971**, *55*, 3647–3650.
(62) Noyes, R. M. *J. Am. Chem. Soc.* **1956**, *78*, 5486–5490.
(63) Reid, A. T. *Biochem. Biophys.* **1952**, *43*, 416–423.
(64) Wolff, R. K.; Bronskill, M. J.; Hunt, J. W. *J. Chem. Phys.* **1970**, *53*, 4211–4215.
(65) Lam, K. Y.; Hunt, J. W. *Int. J. Radiat. Phys. Chem* **1975**, *7*, 317–338.
(66) Jonah, C. D.; Miller, J. R.; Matheson, M. S. *J. Phys. Chem.* **1977**, *81*, 1618–1622.
(67) Peled, E.; Czapski, G. *J. Phys. Chem.* **1971**, *75*, 3626–3630.
(68) Czapski, G.; Peled, E. *J. Phys. Chem.* **1973**, *77*, 893–897.
(69) Ly, A.; Aguilera, J. A.; Milligan, J. R. *Radiat. Phys. Chem.* **2007**, *76*, 982–987.
(70) Milligan, J. R.; Aguilera, J. A.; Ward, J. F. *Radiat. Res.* **1993**, *133*, 158–162.
(71) Milligan, J. R.; Wu, C. C. L.; Ng, J. Y. Y.; Aguilera, J. A.; Ward, J. F. *Radiat. Res.* **1996**, *146*, 510–513.
(72) Elliot, A. J. *Rate Constants and G-Values for the Simulation of the Radiolysis of Light Water over the Range 0−300 °C*; AECL Research, Chalk River Laboratories, Chalk River, Ontario, Canada 1994.
(73) Funston, A. M.; Silverman, E. E.; Schanze, K. S.; Miller, J. R. *J. Phys. Chem. B* **2006**, *110*, 17736–17742.
(74) YamaKawa, H.; Fujii, M. *Macromolecules* **1973**, *6*, 407–415.

JP809413X